Mitigation of Phase Noise in Massive MIMO Systems: A Rate-Splitting Approach

Anastasios Papazafeiropoulos, Bruno Clerckx, and Tharm Ratnarajah

Abstract—This work encompasses Rate-Splitting (RS), providing significant benefits in multi-user settings in the context of huge degrees of freedom promised by massive Multiple-Input Multiple-Output (MIMO). However, the requirement of massive MIMO for cost-efficient implementation makes them more prone to hardware imperfections such as phase noise (PN). As a result, we focus on a realistic broadcast channel with a large number of antennas and hampered by the unavoidable PN. Moreover, we employ the RS transmission strategy, and we show its robustness against PN, since the sum-rate does not saturate at high signal-to-noise ratio (SNR). Although, the analytical results are obtained by means of the deterministic equivalent analysis, they coincide with simulation results even for finite system dimensions.

Index Terms—Rate-splitting, massive MIMO, regularized zeroforcing precoding, phase noise, deterministic equivalent analysis.

I. Introduction

Massive Multiple-Input Multiple-Output (MIMO), known also as large MIMO, is one of the promising technologies for Fifth Generation, (5G) networks [1]. The key concept takes into account the law of large numbers. Specifically, a base station (BS) with a large number of antennas enables fast fading, intracell interference, and additive Gaussian noise to averaged out as the number of antennas tends to infinity [2]–[4].

Inevitable phase noise (PN) occurs in communication systems even after applying calibration and compensation techniques [5]. It is a fundamental bottleneck of wireless communications that cannot be estimated with infinite precision. PN includes phase drifts from the Local Oscillators (LOs) that present a multiplicative nature with regards to the channel vector. Note that phase drifts accumulate within the channel coherence time. PN contributes to inaccurate Channel State Information at the Transmitter (CSIT), and degrades further the spectral efficiency. Moreover, its effect becomes more severe in massive MIMO systems involving a large number of antennas. In fact, the more cost-efficient massive MIMO are, the more prone to hardware impairments, such as PN, are. Actually, PN has been considered in some works such as [6]-[8] to assess the realistic performance of communication systems, but none of them has accounted for its mitigation. Unfortunately,

A. Papazafeiropoulos and T. Ratnarajah are with the Institute for Digital Communications (IDCOM), University of Edinburgh, Edinburgh, EH9 3JL, U.K., (email: a.papazafeiropoulos, t.ratnarajah@ed.ac.uk). B. Clerckx is with the Communications and Signal Processing group in the Department of Electrical and Electronic Engineering, Imperial College London, SW7 2AZ U.K., (email: b.clerckx@imperial.ac.uk.)

This work was supported by the U.K. Engineering and Physical Sciences Research Council (EPSRC) under grants EP/N014073/1 and EP/N015312/1.

the majority of massive MIMO literature has assumed perfect hardware, despite the existence of PN. It is conjectured that if we follow the same path, the gap between theory and practice will increase, and misleading conclusions will be made during the design and evaluation of 5G systems.

This work tackles the challenge of mitigating PN by leveraging the Rate-Splitting (RS) approach. According to RS, we can split one's User-Element (UE) message into a common part and a private part. RS outperforms conventional broadcasting because it does not experience any ceiling effect. Henceforth, we denote by NoRS all the conventional techniques to contrast with the RS technique. We aim at showing the robustness of RS in massive MIMO systems by a deterministic equivalent (DE) analysis, when PN is accounted. In particular, this work shows the robustness of the RS method in realistic Time-Division-Duplex (TDD)-based massive MIMO with PN and imperfect CSIT. Note that both pilot contamination and PN contribute to imperfect CSIT.

The remainder of this paper is structured as follows. Section II presents the system model. Moreover, we present the PN and the RS approach. Next, in Section III, we provide the uplink training phase with PN, while Section IV shows the corresponding downlink transmission. Section V exposes the design of the precoder of the common message, and mainly, the achievable rates in the presence of PN in terms of a DE analysis. The numerical results are placed in Section VI, while Section VII summarizes the paper.

Notation: Vectors and matrices are denoted by boldface lower and upper case symbols. $(\cdot)^{\mathsf{T}}, (\cdot)^{\mathsf{*}}, (\cdot)^{\mathsf{H}},$ and $\operatorname{tr}(\cdot)$ represent the transpose, conjugate, Hermitian transpose, and trace operators, respectively. The expectation operator is denoted by $\mathbb{E}\left[\cdot\right]$. The $\operatorname{diag}\{\cdot\}$ operator generates a diagonal matrix from a given vector, and the symbol \triangleq declares definition. The notations $\mathcal{C}^{M\times 1}$ and $\mathcal{C}^{M\times N}$ refer to complex M-dimensional vectors and $M\times N$ matrices, respectively. Finally, $\mathbf{b}\sim\mathcal{CN}(\underline{0},\mathbf{\Sigma})$ and $\mathbf{b}\sim\mathcal{N}(\underline{0},\mathbf{\Sigma})$ denote a circularly symmetric complex Gaussian variable with zero-mean and covariance matrix $\mathbf{\Sigma}$ and the corresponding real Gaussian variable, respectively.

II. SYSTEM MODEL

We consider a Broadcast (BC) channel, where the BS has M antennas and serves simultaneously K single-antenna UEs. Moreover, we assume that the channel $\mathbf{h}_k \triangleq \left[h_k^1,\dots,h_k^M\right] \in \mathbb{C}^{M\times 1}$ between the BS and UE k is a frequency-flat channel, expressed by

$$\mathbf{h}_k = \mathbf{R}_k^{1/2} \mathbf{w}_k,\tag{1}$$

where $\mathbf{R}_k = \mathbb{E}[\mathbf{h}_k \mathbf{h}_k^{\mathsf{H}}] \in \mathbb{C}^{M \times M}$ is a deterministic Hermitian-symmetric positive-definite matrix representing versatile effects such as the path loss to each antenna. Note that $\mathbf{w}_k \in \mathbb{C}^{M \times 1}$ is an uncorrelated fast-fading Gaussian channel vector drawn as $\mathbf{w}_k \sim \mathcal{CN}(\underline{0}, \mathbf{I}_M)$. Hence, we have that $\mathbf{h}_k \sim \mathcal{CN}(\underline{0}, \mathbf{R}_k)$.

A. Phase Noise

The PN expresses the distortion in the phase due to the random phase drift in the signal coming from the LOs of the BS and UE k, and it is induced during the up-conversion of the baseband signal to passband and vice-versa. Mathematically, it is described by a discrete-time independent Wiener process [6], [9]. Specifically, the PNs at the LOs of the mth antenna of the BS and kth UE are modeled as

$$\phi_{m,n} = \phi_{m,n-1} + \delta_n^{\phi_m} \tag{2}$$

$$\varphi_{k,n} = \varphi_{k,n-1} + \delta_n^{\varphi_k},\tag{3}$$

where $\delta_n^{\phi_m} \sim \mathcal{N}(0,\sigma_{\phi_m}^2)$ and $\delta_n^{\varphi_k} \sim \mathcal{N}(0,\sigma_{\varphi_k}^2)$. Note that $\sigma_i^2 = 4\pi^2 f_{\rm c} c_i T_{\rm s}, \ i = \phi_m, \varphi_k$ describes the PN increment variance with $T_{\rm s}, \ c_i$, and $f_{\rm c}$ being the symbol interval, a constant dependent on the oscillator, and the carrier frequency, respectively.

We assume that the PN processes are considered as mutually independent, if each antenna has its own oscillator, i.e., a Separate Local Oscillator (SLO) at each antenna. In the case that we have just one Common LO (CLO) connected to all BS antennas, there is only one PN process ϕ_n . In our analysis, we focus on both SLOs and CLO scenarios, but in all cases, we assume i.i.d. PN statistics across different antennas and UEs, i.e., $\sigma_{\phi_m}^2 = \sigma_\phi^2$ and $\sigma_{\varphi_k}^2 = \sigma_\varphi^2$, $\forall m, k$.

Actually, the PN is expressed as a multiplicative factor to the channel vector as

$$\tilde{\mathbf{g}}_{k,n} = \mathbf{\Theta}_{k,n} \mathbf{h}_k,\tag{4}$$

where $\Theta_{k,n} \triangleq \operatorname{diag} \left\{ e^{j\theta_{k,n}^{(1)}}, \dots, e^{j\theta_{k,n}^{(M)}} \right\} = e^{j\varphi_{k,n}} \Phi_n \in \mathbb{C}^{M \times M}$ is the total PN with $\Phi_n \triangleq \operatorname{diag} \left\{ e^{j\phi_{1,n}}, \dots, e^{j\phi_{M,n}} \right\}$ being the PN sample matrix at time n because of the imperfections in the LOs of the BS, while, $e^{j\varphi_{k,n}}$ is the PN induced by UE k. Basically, $\tilde{\mathbf{g}}_{k,n}$ represents the effective channel vector at time n. Clearly, the effective channel, given by (4), depends on the time slot of symbol n due to the time-dependence coming from the PN.

B. RS Approach

RS is a very promising method in multi-user transmissions with imperfect CSIT, since it achieves unsaturated sum-rate with increasing SNR despite the presence of imperfect CSIT [10]–[12].

According to this method, the message intended for UE k is split into two parts, namely, a common and a private part. The common part, drawn from a public codebook, should be decoded by all UEs with zero error probability. The private part is to be decoded only by UE k. Note that the messages

intended for the other UEs consist of a private part only. In mathematical terms, we have

$$\mathbf{x} = \underbrace{\sqrt{\rho_c} \mathbf{f}_c s_c}_{\text{common part}} + \underbrace{\sum_{k=1}^K \sqrt{\lambda \rho_k} \mathbf{f}_k s_k}_{private\ part}, \tag{5}$$

where s_c is the common message and s_k is the private message of UE k, while \mathbf{f}_c denotes the precoding vector of the common message with unit norm and \mathbf{f}_k is the linear precoder corresponding to UE k. Note that λ is the normalization parameter regarding the precoder given by

$$\lambda = \frac{K}{\mathbb{E}\left[\operatorname{tr}\mathbf{F}^{\mathsf{H}}\mathbf{F}\right]}.$$
 (6)

According to the decoding procedure, the common message is decoded by each UE, while all private messages are treated as noise. Next, each UE subtracts the contribution of the common message in the received signal and is able to decode its own private message.

III. UPLINK PILOT TRAINING PHASE WITH PN

By assuming TDD, we consider coherence blocks with duration of T channel uses. Each block is split into $\tau \geq K$ uplink pilot symbols and $T-\tau$ downlink data symbols. The CSI is acquired during the uplink training phase, while we exploit channel reciprocity for the downlink channel. During this phase, we assign a pilot sequence of τ symtbols to UE k, i.e., $\omega_k \triangleq [\omega_{k,1},\ldots,\omega_{k,\tau}]^{\mathsf{T}} \in \mathbb{C}^{\tau \times 1}$ with $\rho_{up}^{\mathrm{UE}} = [|\omega_{k,n}|^2], \forall k, n$. Note that the sequences among different UEs are mutually orthogonal.

The received uplink vector at the BS at time $n \in [0, \tau]$ $\mathbf{y}_n^{\mathrm{tr}} \in \mathbb{C}^{M \times 1}$, accounting for the PN, is given by

$$\mathbf{y}_{n}^{\text{tr}} = \sum_{k=1}^{K} \tilde{\mathbf{g}}_{k,n} \omega_{k,n} + \mathbf{z}_{n}^{\text{BS}}, \tag{7}$$

where $\mathbf{z}_n^{\mathrm{BS}} \sim \mathcal{CN}\left(0, \sigma_{\mathrm{BS}}^2 \mathbf{I}_M\right)$ is the Additive White Gaussian Noise (AWGN) at UE k. As mentioned, \mathbf{h}_k is assumed to be constant during the coherence time T, while it changes independently afterwards.

Concatenation of all the received signal vectors during the training phase results in a new vector $\boldsymbol{\psi} \triangleq \left[\mathbf{y}_0^{\mathrm{tr}^{\mathsf{T}}}, \dots, \mathbf{y}_{\tau}^{\mathrm{tr}^{\mathsf{T}}}\right]^{\mathsf{T}} \in \mathbb{C}^{\tau M \times 1}$. Simlar to [13], the Linear Minimum Mean-Square Error (LMMSE) estimate of the channel of UE k during the training phase is given by

$$\hat{\mathbf{g}}_{k,n} = \mathbb{E} \left[\tilde{\mathbf{g}}_{k,n} \boldsymbol{\psi}^{\mathsf{H}} \right] \left(\mathbb{E} \left[\boldsymbol{\psi} \boldsymbol{\psi}^{\mathsf{H}} \right] \right)^{-1} \boldsymbol{\psi}
= \left(\boldsymbol{\omega}_{k}^{\mathsf{H}} \boldsymbol{\Delta}_{k}^{\mathsf{tr}} \otimes \mathbf{R}_{k} \right) \boldsymbol{\Sigma}^{-1} \boldsymbol{\psi},$$
(8)

where

$$\boldsymbol{\Delta}_{k}^{\text{tr}} \triangleq \text{diag}\left\{e^{-\frac{\sigma_{\varphi}^{2} + \sigma_{\phi}^{2}}{2}}, \dots, e^{-\frac{\sigma_{\varphi}^{2} + \sigma_{\phi}^{2}}{2}\tau}\right\}$$
(9)

$$\mathbf{\Sigma} \triangleq \sum_{j=1}^{K} \mathbf{X}_{j} \otimes \mathbf{R}_{j} + \sigma_{\mathrm{BS}}^{2} \mathbf{I}_{\tau M}, \tag{10}$$

$$\mathbf{D}_{|\boldsymbol{\omega}_{j}|^{2}} \triangleq \operatorname{diag}\left(|\omega_{j,1}|^{2}, \dots, |\omega_{j,\tau}|^{2}\right), \tag{11}$$

$$\left[\mathbf{X}_{j}\right]_{u,v} \triangleq \omega_{j,u} \omega_{j,v}^{*} \rho_{up}^{\mathrm{UE}} e^{-\frac{\sigma_{\varphi}^{2} + \sigma_{\phi}^{2}}{2}|u-v|}.$$
 (12)

Proof: The proof is ommited for the sake of limited space.

The LMMSE estimation enables us to write the current channel at the end of the training phase as

$$\tilde{\mathbf{g}}_{k,\tau} = \hat{\mathbf{g}}_{k,\tau} + \mathbf{e}_{k,\tau},\tag{13}$$

where $\mathbf{e}_{k,\tau}$ is the Gaussian distributed zero-mean estimation error vector with covariance given by $\tilde{\mathbf{R}}_k = \mathbf{R}_k - \hat{\mathbf{R}}_k$.

We have
$$\hat{\mathbf{g}}_k \sim \mathcal{CN}\left(\underline{0}, \hat{\mathbf{R}}_k\right)$$
 with $\hat{\mathbf{R}}_k = (\boldsymbol{\omega}_k^{\mathsf{H}} \boldsymbol{\Delta}_k^{\mathsf{tr}} \otimes \mathbf{R}_k) \boldsymbol{\Sigma}^{-1} (\boldsymbol{\Delta}_k^{\mathsf{tr}^{\mathsf{H}}} \boldsymbol{\omega}_k \otimes \mathbf{R}_k)$.

The dependence of the estimated channel on time n necessitates a continuous computation of the applied precoder in the downlink at every symbol interval, which is computationally prohibitive due to its complexity. Therefore, we assume that the precoder is designed by means of the channel estimate once during the training phase and then is applied for the whole duration of the downlink transmission phase. For example, if the channel is estimated at $n_0 = \tau$, the applied precoder is denoted by $\mathbf{f_k} \triangleq \mathbf{f_{k,n_0+1}}$.

IV. DOWNLINK TRANSMISSION UNDER PN

Based on channel reciprocity, the received signal by UE k during the transmission phase $n \in [\tau + 1, T]$ is given by

$$y_{k,n} = \mathbf{h}_k^{\mathsf{H}} \mathbf{\Theta}_{k,n}^* \mathbf{x} + z_{k,n}^{\mathsf{UE}}, \tag{14}$$

where $z_{k,n}^{\rm UE}\sim \left(0,\sigma_{\rm UE}^2\right)$ is the Additive White Gaussian Noise (AWGN) at UE k.

During the downlink transmission phase described by (14), we set $\mathbf{h}_k^{\mathsf{H}} \boldsymbol{\Theta}_{k,\tau}^* = \tilde{\mathbf{g}}_{k,\tau}^{\mathsf{H}}$. If we solve with respect to $\mathbf{h}_k^{\mathsf{H}}$ and make the necessary substitution, we result in

$$\mathbf{h}_{k}^{\mathsf{H}} \mathbf{\Theta}_{k,n}^{*} = \tilde{\mathbf{g}}_{k,\tau}^{\mathsf{H}} \widetilde{\mathbf{\Theta}}_{k,n}. \tag{15}$$

where
$$\widetilde{\Theta}_{k,n} \triangleq \operatorname{diag} \left\{ e^{-j\left(\theta_{k,n}^{(1)} - \theta_{k,\tau}^{(1)}\right)}, \dots, e^{-j\left(\theta_{k,n}^{(M)} - \theta_{k,\tau}^{(M)}\right)} \right\}.$$

Consequently, if we set $\mathbf{g}_{k,n} = \mathbf{\Theta}_{k,n}^* \mathbf{\tilde{g}}_{k,\tau}$ (14) becomes

$$y_{k,n} = \mathbf{g}_{k,n}^{\mathsf{H}} \mathbf{x} + z_{k,n}^{\mathsf{UE}}. \tag{16}$$

The trace T_{PN} of PN is given by

$$T_{\text{PN}} = \operatorname{tr} \widetilde{\boldsymbol{\Theta}}_{k,n}$$

$$= \sum_{l=1}^{M} e^{-j\left(\theta_{k,n}^{(l)} - \theta_{k,\tau}^{(l)}\right)}.$$
(17)

From (17), we get the following useful lemma.

Lemma 1: For CLO and SLOSs, we have

$$\frac{1}{M}T_{\rm PN} \xrightarrow{M \to \infty} \begin{cases} e^{-j\left(\delta^{\phi} + \delta^{\varphi}\right)} & \text{CLO setup} \\ e^{-\frac{\delta_{\phi}^{2}}{2}n - j\delta^{\varphi}} & \text{SLOs setup.} \end{cases}$$
(18)

Proof: The proof is straightforward by means of the application of the law of large numbers.

Remark 1: This lemma describes the effect of PN from both BS and UE LOs.

A. SINR with PN and NoRS (Conventional Transmission)

The SINR of UE k, assuming equal power allocation, is expressed by means of (16) as

$$SINR_{k,n}^{NoRS} = \frac{\frac{\rho_k}{K} \lambda |\mathbf{g}_{k,n}^{\mathsf{H}} \mathbf{f}_k|^2}{\lambda \sum_{j \neq k}^{K} \frac{\rho_j}{K} |\mathbf{g}_{k,n}^{\mathsf{H}} \mathbf{f}_j|^2 + \sigma_{UE}^2}.$$
 (19)

Note that we treat the multi-user interference as independent Gaussian noise (the worst-case assumption) for the calculation of the mutual information [13, Lemma 1].

The mutual information between the received signal and the transmitted symbols is lower bounded by

$$R^{\text{NoRS}} = \sum_{k=1}^{K} R_k^{\text{NoRS}}$$

$$= \frac{1}{T_c} \sum_{k=1}^{K} \sum_{n=1}^{T_c - \tau} R_{k,n}^{\text{NoRS}},$$
(20)

where $R_{k,n}^{\text{NoRS}} = \log_2 (1 + \text{SINR}_{k,n}^{\text{NoRS}})$. In particular, we compute the achievable rate of each UE for each time instance of the data transmission phase as in [6], [13].

B. SINR with PN under RS

We allocate $\rho_{\rm c}=\rho\left(1-t\right)$ to the common message and $\rho_{\rm k}=\rho t/K$ to the private message of each UE, where $t\in(0,1]$. The role of t is to adjust the fraction of the total power spent for the transmission of the private messages.

The SINRs of both common and private messages are given by

$$SINR_{k,n}^{c} = \frac{\rho_c \lambda |\mathbf{g}_{k,n}^{\mathsf{H}} \mathbf{f}_c|^2}{\lambda \sum_{j=1}^{K} \frac{\rho_j}{\beta_k} |\mathbf{g}_{k,n}^{\mathsf{H}} \mathbf{f}_j|^2 + \sigma_{\mathrm{UE}}^2}$$
(21)

$$SINR_n^c = \min_k \left(SINR_{k,n}^c \right) \tag{22}$$

$$SINR_k^p = \frac{\frac{\rho_k}{K} \lambda |\mathbf{g}_{k,n}^{\mathsf{H}} \mathbf{f}_k|^2}{\lambda \sum_{j \neq k}^{K} \frac{\rho_j}{\rho_j} |\mathbf{g}_{k,n}^{\mathsf{H}} \mathbf{f}_j|^2 + \sigma_{UE}^2}.$$
 (23)

The achievable sum-rate is given by

$$R^{RS} = R^{c} + \sum_{j=1}^{K} R_{j}^{p},$$
 (24)

where, similar to (20), we have $R^c = \frac{1}{T_c} \sum_{n=1}^{T_c - \tau} \log_2(1 + \text{SINR}_n^c)$ and $R_j^P = \frac{1}{T_c} \sum_{n=1}^{T_c - \tau} \log_2\left(1 + \text{SINR}_{j,n}^c\right)$ corresponding to the common and private achievable rates, respectively. Note that $\text{SINR}_n^c = \min_k\left(\text{SINR}_{k,n}^c\right)$ and $\text{SINR}_{j,n}^P$ correspond to the common and private SINRs, respectively.

V. DETERMINISTIC EQUIVALENT DOWNLINK PERFORMANCE ANALYSIS WITH PN AND IMPERFECT CSIT

The DEs of the SINRs for NoRS and RS are such that $SINR_{k,n} - \overline{SINR}_{k,n} \xrightarrow[M \to \infty]{a.s.} 0^1$, while the deterministic rate

 $^1 \text{Note that} \ \frac{\text{a.s.}}{M \to \infty} \ \text{denotes almost sure convergence, and} \ a_n \asymp b_n$ expresses the equivalence relation $a_n - b_n \ \frac{\text{a.s.}}{M \to \infty} \ 0$ with a_n and b_n being two infinite sequences.

of UE k is obtained by the dominated convergence [14] and the continuous mapping theorem [15] by means of (20), (24)

$$R_k - \bar{R}_k \xrightarrow[M \to \infty]{\text{a.s.}} 0,$$
 (25)

where $\overline{\text{SINR}}_{k,n}$ and \bar{R}_k are the corresponding DEs. However, in order to present the main results, it is priority to design the precoder for the common message.

A. Precoder Design

The RS method necessitates two types of precoders multiplying the private and common messages, respectively.

1) Precoding of the Private Messages: For the sake of simplicity, we design the precoder of the private message by using RZF in terms of the channel estimate $\hat{\mathbf{G}}_n$. Specifically, we have

$$\mathbf{F}_{n} = \left(\hat{\mathbf{W}} + \operatorname{diag}\left(\hat{\mathbf{W}}\right) + \mathbf{Z} + M\alpha \,\sigma_{\mathrm{BS}}^{2}\mathbf{I}_{M}\right)^{-1}\hat{\mathbf{G}}$$
$$= \mathbf{\Sigma}\hat{\mathbf{G}}, \tag{26}$$

where $\mathbf{\Sigma} \triangleq \left(\hat{\mathbf{W}} + \operatorname{diag}\left(\hat{\mathbf{W}}\right) + \mathbf{Z} + M\alpha \, \sigma_{\mathrm{BS}}^2 \mathbf{I}_M\right)^{-1}$ with $\hat{\mathbf{W}} \triangleq \hat{\mathbf{G}}\hat{\mathbf{G}}^{\mathsf{H}}$. Note that $\mathbf{Z} \in \mathbb{C}^{M \times M}$ is an arbitrary Hermitian nonnegative definite matrix and α is a regularization parameter scaled by M, in order to converge to a constant, as $M, K \to \infty$. Also, α , \mathbf{Z} could be optimized, but this is outside the scope of this paper.

2) Precoding of the Common Message: Herein, we elaborate on the design of the precoder \mathbf{f}_c of the common message in the presence of PN by following a similar procedure to [11]. Specifically, since in the large number of antennas-regime the different channel estimates tend to be orthogonal, we assume that \mathbf{f}_c is written as a linear sum of these channel estimates in the subspace including $\hat{\mathbf{G}}$. Mathematically, this is described by

$$\mathbf{f}_c = \sum_k \alpha_k \hat{\mathbf{g}}_k. \tag{27}$$

The target is the maximization of the achievable rate of the common message $\mathbf{R}_{k,n}^c$. This optimization problem is described by

$$\mathcal{P}_{1} : \max_{\mathbf{f}_{c} \in \mathcal{S}} \min_{k} q_{k} |\mathbf{g}_{k,n}^{\mathsf{H}} \mathbf{f}_{c}|^{2},$$

s.t. $||\mathbf{f}_{c}||^{2} = 1$ (28)

where $q_k = \frac{\rho_c \lambda}{\lambda \sum_{j=1}^K \frac{\rho_j}{K} |\mathbf{g}_{k,n}^{\mathrm{H}} \mathbf{f}_j|^2 + \sigma_{\mathrm{UE}}^2}$. The optimal solution $\{\alpha_k^*\}$ is provided by means of the following proposition. Note that below, we are going to use the DE of T_{PN} , given by Lemma 1.

Proposition 1: In the large system limit, the optimal solution of the practical problem set by \mathcal{P}_1 , where PN is taken into account, is given by

$$\alpha_k^* = \frac{1}{\sqrt{M \sum_{j=1}^K \frac{q_k \frac{1}{M^2} \operatorname{tr}^2 \hat{\mathbf{R}}_k}{q_j \frac{1}{M^2} \operatorname{tr}^2 \hat{\mathbf{R}}_j}}}, \ \forall k.$$
 (29)

Proof: After deriving the DEs of the equation and the constraint of the optimization problem described by \mathcal{P}_1 , we

lead to an optimization problem with deterministic variables. Specifically, applying [3, Thm. 3.7] to (28), we obtain

$$\mathcal{P}_{2} : \max_{\alpha_{k}} \min_{k} q_{k} \frac{1}{M^{2}} |\alpha_{k} \operatorname{tr} \widetilde{\mathbf{\Theta}}_{k,n} \operatorname{tr} \widehat{\mathbf{R}}_{k}|^{2},$$
s.t.
$$\sum_{k} \alpha_{k}^{2} = \frac{1}{M},$$
(30)

where \mathcal{P}_2 includes a complex expression by means of $\widetilde{\Theta}_{k,n}$. Use of Lemma 1 and [3, Thm. 3.7] transforms (30) to

$$\mathcal{P}_3: \max_{\alpha_k} \min_k q_k \alpha_k^2 \frac{1}{M^2} \begin{cases} \operatorname{tr}^2 \hat{\mathbf{R}}_k & \text{CLO setup} \\ e^{-\sigma_\phi^2 n} \operatorname{tr}^2 \hat{\mathbf{R}}_k & \text{SLOs setup,} \end{cases}$$
(31)

$$\text{s.t.} \quad \sum_{k} \alpha_k^2 = \frac{1}{M}. \tag{32}$$

Lemma 2 in [16] concludes the proof by enabling us to show that the optimal solution, satisfying \mathcal{P}_3 , results, if all terms are equal. In such case, we have $q_k\alpha_k^2\frac{1}{M^2}\begin{cases} \operatorname{tr}^2\hat{\mathbf{R}}_k=q_j\alpha_j^2\frac{1}{M^2}\operatorname{tr}^2\hat{\mathbf{R}}_j & \text{CLO setup}\\ e^{-\sigma_\phi^2 n}\operatorname{tr}^2\hat{\mathbf{R}}_k=q_j\alpha_j^2\frac{1}{M^2}e^{-\sigma_\phi^2 n}\operatorname{tr}^2\hat{\mathbf{R}}_j & \text{SLOs setup},\\ \forall k\neq j & & \blacksquare \end{cases}$

B. Achievable Deterministic Sum-Rate with RS in the Presence of PN with Imperfect CSIT

In this section, we conduct a DE analysis of a practical system with PN for both the RS and the NoRS strategies. Specifically, we derive the DE of the kth UE in the asymptotic limit of K, M for fixed ratio $\beta = K/M$.

Theorem 1: The downlink DEs of the SINRs of UE k at time n corresponding to the private and common messages with RZF precoding in the presence of PN and imperfect CSIT, are given by

$$\overline{\text{SINR}}_{k}^{\text{p}} = \frac{\frac{\rho_{k}}{K} \overline{\lambda} \left(\frac{\frac{1}{M} \operatorname{tr} \widetilde{\Theta}_{k,n} \delta_{k}}{1 + \delta_{k}}\right)^{2}}{\overline{\lambda} \sum_{j \neq k}^{K} \frac{\rho t}{K} \frac{Q_{jk}}{M(1 + \delta_{j})^{2}} + \sigma_{\text{UE}}^{2}}$$
(33)

$$\overline{\text{SINR}}_{k}^{c} = \frac{\rho_{c}\bar{\lambda}\left(\alpha_{k}\frac{1}{M}\operatorname{tr}\widetilde{\boldsymbol{\Theta}}_{k,n}\frac{1}{M}\operatorname{tr}\widehat{\mathbf{R}}_{k}\right)^{2}}{\bar{\lambda}\frac{\rho t}{K}\left(\frac{1}{M}\operatorname{tr}\widetilde{\boldsymbol{\Theta}}_{k,n}\delta_{k}}{1+\delta_{k}}\right)^{2} + \sum_{j\neq k}^{K}\frac{\rho t}{K}\frac{Q_{jk}}{M(1+\delta_{j})^{2}} + \sigma_{\text{UE}}^{2}}.$$
(34)

where

$$\bar{\lambda} = K \left(\frac{1}{M} \sum_{k=1}^{K} \frac{\delta_{k}^{'}}{\left(1 + \delta_{k}\right)^{2}} \right)^{-1},$$

and

$$Q_{jk} \approx \frac{\delta_j''}{M} + \frac{\left|\delta_k''\right|^2 \delta_k''}{M \left(1 + \delta_j\right)^2} - 2\operatorname{Re}\left\{\frac{\frac{1}{M}\operatorname{tr}\widetilde{\boldsymbol{\Theta}}_{k,n}\delta_k \delta_k''}{M \left(1 + \delta_j\right)}\right\}. \tag{35}$$

(29) Also, we have $\delta_k = \frac{1}{M} \operatorname{tr} \hat{\mathbf{R}}_k \mathbf{T}$, $\delta_k' = \frac{1}{M} \operatorname{tr} \hat{\mathbf{R}}_k \hat{\mathbf{T}}'$, $\delta_j' = \frac{1}{M} \operatorname{tr} \hat{\mathbf{R}}_j \hat{\mathbf{T}}'$, $\delta_k = \frac{1}{M} \operatorname{tr} \hat{\mathbf{R}}_k \hat{\mathbf{T}}'$, $\mathbf{S} = \left(\kappa_{\text{\tiny TUE}}^2 \operatorname{diag} \left(\hat{\mathbf{R}}_k\right) + \mathbf{Z}\right) / M$, and $\tilde{a} = \alpha \sigma_{\text{\tiny UE}}^2$ where

* $\mathbf{T} = \mathbf{T}(\tilde{a})$ and $\boldsymbol{\delta} = [\delta_1, \dots, \delta_K]^{\mathsf{T}} = \boldsymbol{\delta}(\tilde{a}) = \boldsymbol{e}(\tilde{a})$ are

given by [17, Theorem 1] for $\mathbf{S} = \mathbf{S}$, $\mathbf{D}_k = \tilde{\kappa}_{\text{rBS}} \hat{\mathbf{R}}_k \ \forall k \in \mathcal{K}$,

- * $\mathbf{T}' = \mathbf{T}'(\tilde{a})$ is given by [3, Theorem 2] for $\mathbf{S} = \mathbf{S}$,
- $$\begin{split} \mathbf{K} &= \mathbf{I}_{M}, \mathbf{D}_{k} = \tilde{\kappa}_{\mathrm{r_{BS}}} \hat{\mathbf{R}}_{k}, \forall k \in \mathcal{K}, \\ * & \mathbf{T}^{''} = \mathbf{T}^{''}(\tilde{a}) \text{ is given by [3, Theorem 2] for } \mathbf{S} = \mathbf{S}, \end{split}$$
 $\mathbf{K} = \hat{\mathbf{R}}_k, \, \mathbf{D}_k = \tilde{\kappa}_{r_{\mathrm{BS}}} \hat{\mathbf{R}}_k, \forall k \in \mathcal{K}.$

Proof: Herein, we shall omit the proof of Theorem 1, which is provided in [18] due to limited space.

Remark 2: Clearly, the PN affects both the numerator and the denominator of the SINRs by putting an extra penalty to the quality of the system. Its increase results in an obvious decrease of the numerator, and an increase of the denominator by means of an increase of Q_{ik} .

C. Power Allocation

The optimal t is rather intricate to find it by maximizing (24) after calculating its first derivative. Thus, we present a suboptimal, but effective solution by following [11]. Specifically, we seek to fulfill the condition allowing RS to outperform the conventional multi-user broadcasting. This condition is accomplished by allocating a fraction t of the total power for the transmission of the private messages RS to guarantee the realization of almost the same sum-rate as the conventional BC with full power. The remaining power is exploited to transmit the common message, which will enable RS to boost the sumrate at high-SNR. The sum-rate payoff of the RS strategy over the conventional BC (NoRS) is determined by the difference

$$\Delta R = R^{c} + \sum_{k=1}^{K} \left(R_{k}^{p} - R_{k}^{NoRS} \right). \tag{36}$$

The necessary condition and the power splitting ratio tto achieve the outperformance are given by the following proposition.

Proposition 2: We can write

$$R_k^{\rm p} \le R_k^{\rm NoRS}. \tag{37}$$

The equality holds when the power splitting ratio t is given by

$$t = \min\left\{\frac{K^2 M}{\bar{\lambda} \sum_{j \neq k}^{K} \frac{\rho Q_{jk}}{(1+\delta_j)^2}}, 1\right\},\tag{38}$$

where $\bar{m}_k = \operatorname{tr} \hat{\mathbf{R}}_k$. As a result, the sum-rate gain ΔR becomes

$$\Delta R \ge R^{c} - \log_2 e. \tag{39}$$

Proof: See Appendix A.

Remark 3: According to (38), increasing the severity of the PN results in less power allocated to the private messages. Interestingly, at high SNR ρt becomes independent of ρ , while the sum-rate increases with the available transmit power by assigning the remaining power $\rho - \rho t$ to the common message. On the contrary at low SNR, t = 1, which means that the common message becomes useless. In such case, broadcasting of only private messages takes place and RS degenerates to NoRS. Generally, by increasing the PN, RS exhibits more its robustness.

VI. NUMERICAL RESULTS

This section presents the numerical illustrations of the analytical and Monte Carlo simulation results obtained for both cases of perfect and imperfect CSIT. Specifically, the bullets represent the simulation results. The black line depicts the ideal sum-rate with RZF and no common message (NoRS), i.e., perfect CSIT and hardware are assumed. The red and cyan as well as the blue and green lines show the sum-rate with NoRS as well as RS when perfect, imperfect CSIT are assumed, respectively. The discrimination between "solid" and "dot" lines designates the results with SLOs and CLO, respectively.

We consider a cell of 250 m \times 250 m with K=2 UEs, where the randomly selected UE is found at a distance of 25m from the BS. The pilot length is B=2. Moreover, we assume a Rayleigh block-fading channel by taking into consideration that the coherence time and the coherence bandwidth are $T_c = 5 \text{ ms}$ and $B_c = 100$ KHz, respectively. As a result, the coherence block consists of T=500 channel uses. In each block, we assume fast fading by means of $\mathbf{w}_k \sim \mathcal{CN}(0, \mathbf{I}_M)$. Also, we set $\mathbf{R}_k = \mathbf{\Lambda}_k$, i.e., we account for path-loss and shadowing, where Λ_k is a $M \times M$ diagonal matrix with elements across the diagonal modeled as [13]

$$\lambda_k^m = \frac{10^{s_k^m - 1.53}}{\left(d_k^m\right)^{3.76}},\tag{40}$$

where d_k^m is the distance in meters between the receive antenna m and UE k, while $s_k^m \sim \mathcal{N}\left(0, 3.16\right)$ represents the shadowing

The power of the uplink training symbols is $ho_{up}^{\mathrm{UE}}=2~\mathrm{dB}$ and the variance of thermal noise is assumed $\sigma_{\mathrm{BS}}^{2}=\sigma_{\mathrm{UE}}^{2}=$ -174 dBm/Hz. Moreover, the PN is simulated as a discrete Wiener process with specific increment variance, and for the sake of simulations, we have set that the nominal values of the uplink PN equal to the downlink PN, e.g., the receive PN at the BS equals to the transmit PN at the BS.

A. Impact of Hardware Impairments on NoRS/RS-Comparisons

In the following figures, the metric under investigation is the DE sum-rate in the cases of both NoRS and RS strategies. The theoretical curves for the cases with imperfect are obtained by means of Theorems 1, while the simulated curves are obtained by averaging the corresponding SINRs over 10³ random channel instances. Note that the curves corresponding to perfect CSIT have been obtained, if we assume no channel estimation phase, but PN is assumed only in the downlink stage. Clearly, as can be shown from the figures, although the DEs are derived for $M, K \to \infty$ with a given ratio, the corresponding results concur with simulations for finite values of M, K^2 . Note that t used in the simulation is obtained by means of both exhaustive search and Proposition 2 for verification.

Fig. 1 provides the comparison of the sum-rate versus the SNR in both cases of perfect and imperfect CSIT by considering M=100 and T=500, while the PN is taken into account on

²Herein and without loss of generality, we consider the overall impact of the PN. Specifically, we add up both PN contributions coming from BS CLO/SLOs and UE LO.

both the uplink and the downlink. The sum-rate with NoRS under perfect CSI and ideal hardware monotonically increases with the increase in the value of ρ . In the practical case where the PN is considered, NoRS saturates after a certain value of SNR in cases of perfect (no PN and no imperfect CSIT at the uplink stage) and imperfect CSIT. Remarkably, RS proves to be robust, since the sum-rate does not saturate. Moreover, when imperfect CSIT is assumed, the degradation of the sum-rate in all cases is obvious. Notably, the setting with SLOs behaves better than the BS architecture with CLO because in such case the phase drifts are independent and in the large system limit they are averaged [13]. Of course, the employment of many LOs (SLOs) results in higher deployment cost. In the presence of PN, RS mitigates the multi-user interference. Thus, we have no saturation.

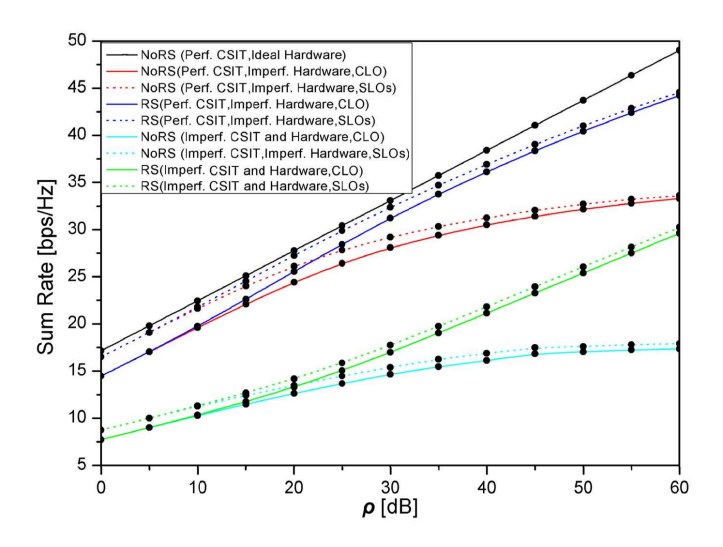


Fig. 1. Sum-rate versus ρ ($M=100,~K=2,~T=500,~\delta=10^{-4},~\kappa^2=0$).

Fig. 2 presents the comparison of the sum-rate versus the SNR after decreasing the number of BS antennas to M/5=20, while Fig. 3 shows the impact of the coherence time T, when it is decreased to T/5=100 channel uses. In other words, in both cases we have an equivalent decrease of 1/5 of M and T. From the former figure, we conclude a decrease of the sum-rate due to the corresponding decrease of M, as expected. Furthermore, the difference between the SLOs and CLO setups now is smaller because we have less independent LOs. The latter figure exposes that a decrease regarding the number of channel uses results in a small decrease of the sum-rate with the saturation in the case of NoRS taking place earlier. Also, the gap between the sum-rates with CLO and SLOs setups is smaller now.

Figs. 4(a) and 4(b) illustrate the sum-rate versus the total PN coming from the BS CLO/SLOs and the LOs of the UEs for $\rho=5~\mathrm{dB}$ and $\rho=25~\mathrm{dB}$, respectively. According to both figures, it can be noted that the various sum-rates decrease monotonically with δ , however, in the first figure, where the SNR is small, there is no improvement coming from the implementation of RS. Hence, the NoRS lines coincide with the respective lines corresponding to the RS strategy. Obviously, the expected

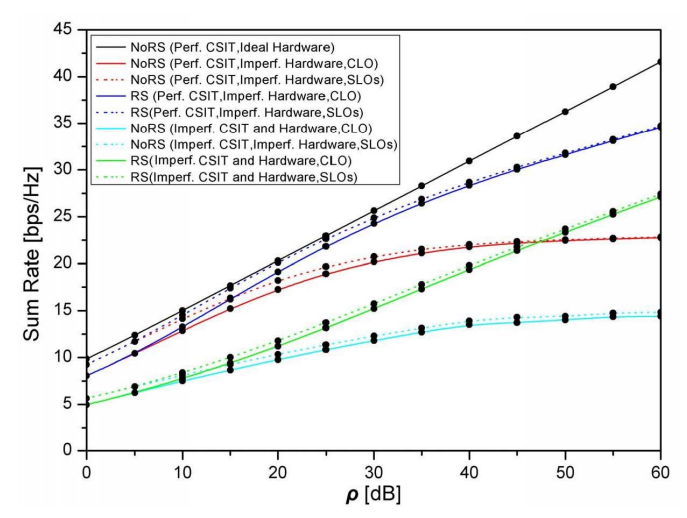


Fig. 2. Sum-rate versus ρ (M = 20, K = 2, T = 500, $\delta = 10^{-4}$).

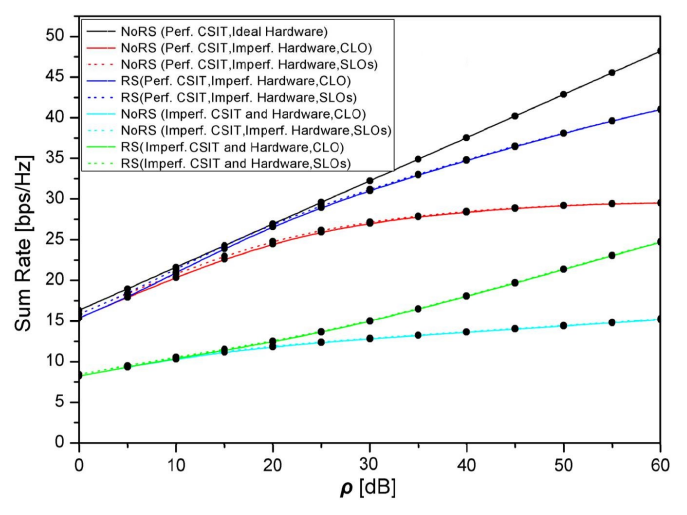
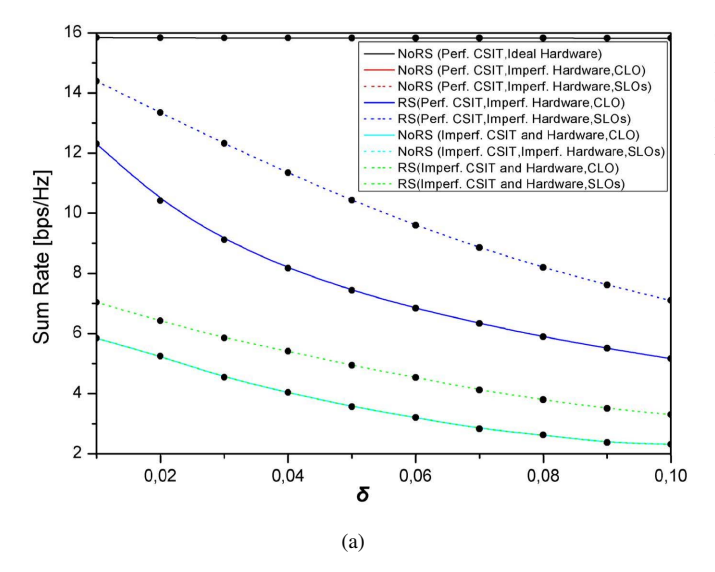


Fig. 3. Sum-rate versus ρ ($M = 100, K = 2, T = 100, \delta = 10^{-4}$).

improvement appears in the second figure, where a higher SNR is assumed. Moreover, as δ decreases, the gap between the sum-rates corresponding to the SLOs and CLO setups narrows because the degradation coming from the accumulation of PN decreases.

VII. CONCLUSIONS

PN is inherent in any communication system. At the same time, the rate of multi-user systems saturates in the cases of imperfect CSIT with PN. For this reason, RS was proposed to tackle the degradation from the multi-user interference induced by imperfect CSIT. In particular, we extended the RS method to the large system regime. We pursued the DE analysis and obtained the downlink achievable rate after designing the precoders for the common and private messages. Remarkably, RS proved to be robust in the case of PN. Moreover, simulations validated the results and showed their applicability even for finite system dimensions.



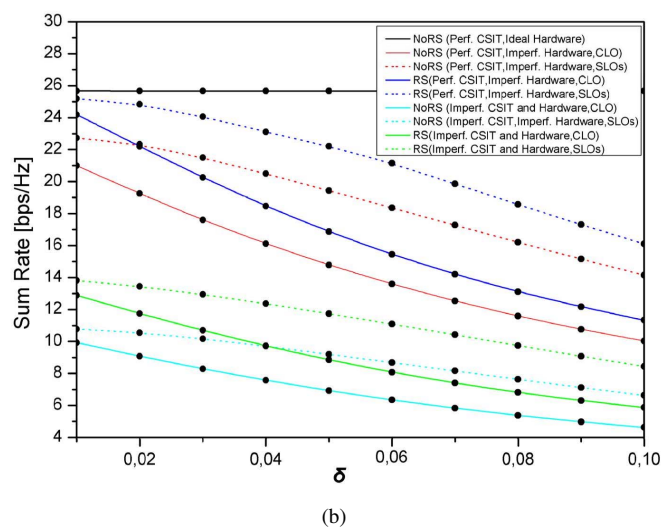


Fig. 4. (a) Sum-rate versus δ ($M=100,\,K=2,\,T=500,\,\rho=5$ dB). (b) Sum-rate versus δ ($M=100,\,K=2,\,T=500,\,\rho=25$ dB).

APPENDIX A PROOF OF PROPOSITION 2

First, we denote $\bar{Y} = \frac{\rho t \bar{\lambda}}{KM} \sum_{j \neq k}^K \frac{Q_{jk}}{(1+\delta_j)^2}$. If $\bar{Y} > 1$, the private part of RS achieves the same sum-rate as the conventional multi-user BC with full power, which means that the equality in (37) nearly holds. Since the common message should be decoded by all UEs, it is reasonable to allocate less power to the common message, as their number increases because the rate of the common decreases, i.e., the benefit of common message reduces. Thus, during the power allocation for the common message, the number of UEs should be taken into account. Moreover, following a similar rationale as in [11], we set $\bar{Y} > K$. We have

$$t = \frac{K^2 M}{\bar{\lambda} \sum_{j \neq k}^{K} \frac{\rho Q_{jk}}{(1 + \delta_j)^2}}.$$
(41)

If we choose t as the smaller value between (41) and 1, the inequality in (37) becomes equality. In the low-SNR regime $\rho \to 0$, (38) gives t = 1. In other words, transmission of the

common message is not beneficial at this regime. However, increasing the SNR, the transmission of the common message enhances the sum-rate, when the sum-rate due to only private messages tends to saturate. If we upper bound the rate loss between the private messages of the NoRS and RS, we obtain similar to [11]

$$\sum_{j=1}^{K} \left(\mathbf{R}_{j}^{\text{NoRS}} - \mathbf{R}_{j}^{\mathbf{p}} \right) \le \log_{2} e. \tag{42}$$

REFERENCES

- "FP7 integrating project METIS (ICT 317669)." [Online]. Available: https://www.metis2020.com
- [2] F. Rusek et al., "Scaling up MIMO: Opportunities and challenges with very large arrays," *IEEE Signal Processing Mag.*, vol. 30, no. 1, pp. 40–60, Jan 2013.
- [3] J. Hoydis, S. ten Brink, and M. Debbah, "Massive MIMO in the UL/DL of cellular networks: How many antennas do we need?" *IEEE J. Select. Areas Commun.*, vol. 31, no. 2, pp. 160–171, February 2013.
- [4] A. K. Papazafeiropoulos and T. Ratnarajah, "Deterministic equivalent performance analysis of time-varying massive MIMO systems," *IEEE Trans. on Wireless Commun.*, vol. 14, no. 10, pp. 5795–5809, 2015.
- [5] C. Studer, M. Wenk, and A. Burg, "MIMO transmission with residual transmit-RF impairments," in *ITG/IEEE Work. Smart Ant. (WSA)*. IEEE, 2010, pp. 189–196.
- [6] A. Pitarokoilis, S. Mohammed, and E. Larsson, "Uplink performance of time-reversal MRC in massive MIMO systems subject to phase noise," *IEEE Trans. Wireless Commun.*, vol. 14, no. 2, pp. 711–723, Feb 2015.
- [7] R. Krishnan et al., "Linear massive MIMO precoders in the presence of phase noise–a large-scale analysis," accepted in IEEE Trans. on Veh. Tech., 2015. [Online]. Available: http://arxiv.org/abs/1501.05461
- [8] A. Papazafeiropoulos, "Impact of general channel aging conditions on the downlink performance of massive MIMO," accepted in IEEE Trans. on Veh. Tech., 2016. [Online]. Available: http://arxiv.org/abs/1605.07661
- [9] A. Demir, A. Mehrotra, and J. Roychowdhury, "Phase noise in oscillators: A unifying theory and numerical methods for characterization," *IEEE Trans. Circuits Syst. I*, vol. 47, no. 5, pp. 655–674, May 2000.
- [10] C. Hao, Y. Wu, and B. Clerckx, "Rate analysis of two-receiver MISO broadcast channel with finite rate feedback: A rate-splitting approach," *IEEE Trans. on Commun.*, vol. 63, no. 9, pp. 3232–3246, 2015.
- [11] M. Dai et al., "A rate splitting strategy for massive MIMO with imperfect CSIT," IEEE Trans. on Wirel. Commun., vol. PP, no. 99, pp. 1–1, 2016.
- [12] B. Clerckx et al., "Rate splitting for MIMO wireless networks: A promising PHY-layer strategy for LTE evolution," *IEEE Communications Magazine*, vol. 54, no. 5, pp. 98–105, 2016.
- [13] E. Björnson, M. Matthaiou, and M. Debbah, "Massive MIMO with nonideal arbitrary arrays: Hardware scaling laws and circuit-aware design," *IEEE Trans. Wireless Commun.*, vol. 14, no. no.8, pp. 4353–4368, Aug. 2015.
- [14] P. Billingsley, Probability and measure, 3rd ed. John Wiley & Sons, Inc., 2008.
- [15] A. W. van der Vaart, Asymptotic statistics (Cambridge series in statistical and probabilistic mathematics). New York: Cambridge University Press, 2000.
- [16] Z. Xiang, M. Tao, and X. Wang, "Massive MIMO multicasting in noncooperative cellular networks," *IEEE Journal on Sel. Areas in Commun.*, vol. 32, no. 6, pp. 1180–1193, 2014.
- [17] S. Wagner et al., "Large system analysis of linear precoding in correlated MISO broadcast channels under limited feedback," *IEEE Trans. Inform. Theory*, vol. 58, no. 7, pp. 4509–4537, July 2012.
- [18] A. Papazafeiropoulos, B. Clerckx, and T. Ratnarajah, "Rate-Splitting to mitigate residual transceiver hardware impairments in massive MIMO," submitted, available upon request, 2016.